Low Temperature Physics/Fizika Nizkikh Temperatur, 2016, v. 42, No. 6, pp. 596–599

Thermoelectric amplification of phonons in graphene

K.A. Dompreh[1], N.G. Mensah[2], S.Y. Mensah[1], and S.K. Fosuhene[3]

[1]*Department of Physics, College of Agriculture and Natural Sciences, University of Cape Coast, Ghana*

[2]*Department of Mathematics, College of Agriculture and Natural Sciences, University of Cape Coast, Ghana*

[3]*Ghana Space Science and Technology Institute, Ghana Atomic Energy Commission, Ghana*

E-mail: kwadwo.dompreh@ucc.edu.gh

Received October 28, 2015, revised February 2, 2016, published online April 25, 2016

Amplification of acoustic in-plane phonons due to an external temperature gradient (∇T) in single-layer graphene (SLG) was studied theoretically. The threshold temperature gradient $(\nabla T)_0^g$ and the threshold voltage $(V_T)_0^g$ in SLG were evaluated. For T = 77 K, the calculated value for $(\nabla T)_0^g$ = 746.8 K/cm and $(V_T)_0^g$ = 6.6 mV. The calculation was done in the hypersound regime. Further, the dependence of the normalized amplification (Γ/Γ_0) on the frequency ω_q and $\nabla T/T$ were evaluated numerically and presented graphically. The calculated threshold temperature gradient $(\nabla T)_0^g$ for SLG was higher than that obtained for homogeneous semiconductors (*n*-InSb) $(\nabla T)_0^{\text{hom}} \approx 10^3$ K/cm, superlattices $(\nabla T)_0^{SL}$ = 384 K/cm, and cylindrical quantum wire $(\nabla T)_0^{cqw} \approx 10^2$ K/cm. This makes SLG a much better material for thermoelectric phonon amplification.

PACS: 73.22.Pr Electronic structure of graphene;
79.10.–n Thermoelectronic phenomena;
63.22.Rc Phonons in graphene.

Keywords: thermoelectric, graphene, acoustic phonon, amplification.

Introduction

The successful exfoliation of SLG sheets has attracted lots of research due to its unusual material properties such as the high carrier mobilities, unusual transport phenomena characteristic for two-dimensional Dirac fermions [1], the anomalous integer quantum Hall effect and Shubnikov–de Haas oscillations that exhibit a phase shift of π due to Berry's phase [2]. SLG is characterized by vibrations of two types of phonons: 1) in-plane vibrations with linear and longitudinal acoustic branches (LA and TA), and 2) out-of-plane vibrations known as flexural phonons (ZA and ZO) [3]. In SLG, these two forms of phonon differ in their coupling to charge carriers: while the coupling is conventional for in-plane phonons; reflection symmetry demands out-of-plane displacement for flexurals phonons. Moreover, scattering of Dirac fermions by flexural phonons requires absorption (or emission) of two phonons which is quadratic in nature whilst the in-plane phonons have linear dispersion. Due to the flexibility of SLG, its flexural mode (also called the ZA mode, bending mode, or out-of-plane transverse acoustic mode) can not be ignored. SLG is 2D material with an in-plane symmetry thus only in-plane phonons modes can couple linearly to electrons [4]. The amplification (absorption) of acoustic phonons in graphene [5–7] and other low-dimensional materials such as superlattices [8–11], carbon nanotubes (CNT) [12] and cylindrical quantum wires (CQW) [12] has attracted lots of attention recently. For SLG, Nunes and Fonseca [7] studied amplification of acoustic phonons and determined the drift velocity V_D at which amplification occurs but Dompreh *et al.* [14] further showed that even at $V_D = 0$, absorption of acoustic phonons can occur. Acoustoelectric effect (AE) involves the transfer of momentum from phonons to conducting charge carriers which leads to the generation of dc current in the sample. This has been studied both theoretically [14,15] and experimentally [16] in graphene. The interaction between electrons and phonons in the presence of an external temperature gradient (∇T) can lead to thermoelectric effect [17–20] and thermoelectric amplification of phonons. Thermoelectric amplification of phonons has been studied in bulk [21,22] and low-dimensional materials such as cylindrical quantum wire (CQW) [23] and superlattices [24]. This phenomena was predicted by Gulyeav (1967) [21] but was thoroughly developed by Sharma and Singh (1974) [25] from a hydrodynamic approach $ql << 1$ (q is the acoustic wave number, l is the electron mean free path). Epstein further explained this effect for sound in the opposite limiting case, $ql >> 1$ and showed that amplification is also possible in an electrically open-circuited sample (i.e., in the absence of an electric

current) [26]. In *n*-InSb, Epstein calculated a threshold temperature gradient of $\approx 10^3$ K/cm at 77 K. However, in superlattices, Mensah and Kangah (1991) [27] calculated the threshold temperature gradient necessary for amplification to occur to be $(\nabla T)_0^{\text{hom}} = 2.6(\nabla T)_0^{SL}$ (where $(\nabla T)_0^{SL}$ is the threshold temperature gradient of superlattice) but in the lowest energy mini-band ($\Delta = 0.1\,\text{eV}$) obtained $(\nabla T)_0^{SL} = 384\,\text{K/cm}$. In all these materials, the threshold temperature gradient for the amplification was found to depend on the scattering mechanism and sound frequency where the relaxation time is independent of energy [24].

Graphene differs significantly from the other low-dimensional materials. It has the highest value for thermal conductivity at room temperature (≈ 3000–5000 W/mK) [28]. This extremely high thermal conductivity opens up a variety of applications. The most interesting property of graphene is its linear energy dispersion $\varepsilon(k) = \pm\hbar V_F\,|\,k\,|$ (the Fermi velocity $V_F \approx 10^8$ cm/s) at the Fermi level with low-energy excitation. Conductivity in SLG is restricted by scattering of impurities but in the absence of extrinsic scattering sources, in-plane phonons constitute an intrinsic source of scattering of electrons to produce measurable temperature gradient (∇T) [25]. In the works of Mariani *et al*. [3], the threshold temperature below which flexural phonons or above which in-plane phonons dominate was calculated to be T = 70 K. To date, there is no study of thermoelectric amplification of acoustic phonons in SLG. In this paper, thermoelectric amplification of acoustic phonons is theoretically studied in SLG with degenerate energy dispersion. Here the threshold temperature gradient $(\nabla T)_0^g$ above which amplification occur is calculated in the regime $ql >> 1$. The paper is organized as follows: In the theory section, the equation underlying the thermoelectric amplification of acoustic phonon in graphene is presented. In the numerical analysis section, the final equation is analyzed and presented in a graphical form. Lastly, the conclusion is presented in Sec. 4.

Theory

The kinetic equation for the acoustic phonon population $N_{\mathbf{q}}(t)$ in the graphene sheet is given by

$$\frac{\partial N_{\mathbf{q}}(t)}{\partial t} = \frac{2\pi}{\hbar} g_s g_v \sum_{\mathbf{k},\mathbf{k}'} |C_{\mathbf{q}}|^2 \delta_{\mathbf{k}',\mathbf{k}} \{[N_{\mathbf{q}}(t)+1] f_{\mathbf{k}} (1- f_{\mathbf{k}'}) \times$$

$$\times \delta(\varepsilon_{\mathbf{k}'} - \varepsilon_{\mathbf{k}} + \hbar\omega_{\mathbf{q}}) - N_{\mathbf{q}}(t)\, f_{\mathbf{k}'}(1- f_{\mathbf{k}})\delta(\varepsilon_{\mathbf{k}'} - \varepsilon_{\mathbf{k}} - \hbar\omega_{\mathbf{q}})\}. \tag{1}$$

Here, we have ignored other processes rather than phonon emission or absorption by electrons. The $g_s = g_v = 2$ account for the spin and valley degeneracy, respectively, $N_{\mathbf{q}}(t)$ represent the number of phonons with a wave vector $\mathbf{q}$ at time t. The factor $N_{\mathbf{q}} + 1$ accounts for the presence of $N_{\mathbf{q}}$ phonons in the system when the additional phonon is emitted. The $f_{\mathbf{k}}(1- f_{\mathbf{k}})$ represent the probability that the initial $\mathbf{k}$ state is occupied and the final electron state $\mathbf{k}'$ is empty whilst the factor $N_{\mathbf{q}} f_{\mathbf{k}'}(1- f_{\mathbf{k}})$ is that of the boson and fermions statistics. From [29], the matrix element $|C_q|$ in Eq. (1) is given as

$$|C_q| = \begin{cases} \sqrt{\dfrac{\Lambda^2 q}{2\rho V_s}} & \text{acoustic phonons,} \\ \sqrt{\left(\dfrac{2\pi^2\rho\omega_0}{q^2}\right)(k_\infty^{-1} - k_0^{-1})} & \text{optical phonons,} \end{cases}$$

where Λ is the deformation potential constant, ρ is the crystal density, V_s is the sound velocity, ω_0 is the frequency of an optical phonon, k_∞^{-1} and k_0^{-1} are, respectively, the low frequency and optical permeabilities of the crystal. In Eq. (1), the summation over k and k' can be transformed into integrals by the prescription

$$\sum_{k,k'} \to \frac{A^2}{(2\pi)^4} \int d^2k d^2k',$$

where A is the area of the sample. Assuming that $N_q(t) >> 1$ yields

$$\frac{\partial N_{\mathbf{q}}}{\partial t} = \Gamma_{\mathbf{q}} N_{\mathbf{q}}, \tag{2}$$

where

$$\Gamma_q = \frac{A|\Lambda|^2\,\hbar q}{(2\pi)^3 \hbar V_F \rho V_s} \int_0^\infty k dk \int_0^\infty k' dk' \int_0^{2\pi} d\varphi \int_0^{2\pi} d\theta \{[f(k) - f(k')] \times$$

$$\times \delta(k - k' - \frac{1}{\hbar V_F}(\hbar\omega_q))\} \tag{3}$$

with

$$k' = k - \frac{1}{\hbar V_F}(\hbar\omega_q),$$

ρ is the density of the graphene sheet, $f(k)$ is the distribution function and V_s is the velocity of sound. Here the acoustic wave will be considered as phonons of frequency (ω_q) in the short-wave region. The linear approximation of the distribution function $f(k)$ is given as

$$f(k) = f_0(\varepsilon(k)) + f_1(\varepsilon(k)), \tag{4}$$

$f_1(k)$ is derived from the Boltzmann transport equation as

$$f_1(\varepsilon(k)) = \tau[(\varepsilon(k) - \xi)\frac{\nabla T}{T}]\frac{\partial f_0(p)}{\partial \varepsilon} v(k). \tag{5}$$

Here $v(k) = \partial\varepsilon(k)/\hbar\partial k$ is the electron velocity, ξ is the chemical potential, τ is the relaxation time and ∇T is the temperature gradient. The unperturbed electron distribution function is given by the shifted Fermi–Dirac function,

$$f_0(k) = \{\exp(\beta\varepsilon(k) - \beta\varepsilon_F) + 1\}^{-1}, \tag{6}$$

where $\beta = 1/k_B T$ (k_B is the Boltzmann constant, T is the absolute temperature and ε_F is the Fermi energy). At low temperatures ($k_B T << 1$), $\varepsilon_F = \xi$, the Fermi–Dirac equilibrium distribution function become

$$f_0(\varepsilon(k)) = \exp(-\beta(\varepsilon(k) - \xi)). \quad (7)$$

Inserting Eqs. (5), (6) and (7) into Eq. (4) and setting $\xi = 0$ for intrinsic graphene, gives

$$\Gamma = \frac{A|\Lambda|^2 \hbar q}{(2\pi)^3 V_F \rho V_s} \int_0^\infty (k^2 - \frac{k\hbar\omega_q}{\hbar V_F})\{\exp(-\beta(\hbar V_F k)) -$$

$$-\beta\hbar V_F \tau(\hbar V_F k)\frac{\nabla T}{\hbar T}\exp(-\beta\hbar V_F k) - \exp(-\beta\hbar V_F (k - \frac{\hbar\omega_q}{\hbar V_F})) -$$

$$-\beta\hbar V_F \tau(\hbar V_F (k - \frac{\hbar\omega_q}{\hbar V_F}))\frac{\nabla T}{\hbar T}\exp(-\beta\hbar V_F (k - \frac{\hbar\omega_q}{\hbar V_F}))\}. \quad (8)$$

Using standard integrals in Eq. (8) and after cumbersome calculations yield the final equation as

$$\Gamma = \Gamma_0\{(2 - \beta\hbar\omega_q)(1 - \exp(-\beta\hbar\omega_q)) -$$

$$-\tau V_F [6(1 + \exp(\beta\hbar\omega_q)) - \beta\hbar\omega_q(2 + \beta\hbar\omega_q \exp(\beta\hbar\omega_q))]\frac{\nabla T}{T}\}, \quad (9)$$

where

$$\Gamma_0 = \frac{2A|\Lambda|^2 q}{2\pi\beta^3\hbar^3 V_F{}^4 \rho V_s}. \quad (10)$$

In Eq. (9), the temperature-dependent parameter is the diffusion coefficient. Increasing temperature increases the particle kinetic energy and the diffusion component of the system. The threshold temperature gradient $(\nabla T)_0^g$ necessary for diffusion to occur is calculated by letting $\Gamma = 0$ as a consequence of the laws of conservation which yields

$$(\nabla T)_0^g = $$

$$= T\frac{(2 - \beta\hbar\omega_q)(1 - \exp(-\beta\hbar\omega_q))}{\tau V_F [6(1 + \exp(\beta\hbar\omega_q)) - \beta\hbar\omega_q(2 + \beta\hbar\omega_q \exp(\beta\hbar\omega_q))]}. \quad (11)$$

The $(\nabla T)_0^g$ is dependent on the temperature (T), the frequency (ω_q) and the relaxation time (τ) as well as the acoustic wavenumber (q). The threshold voltage $(V_T)_0^g$ in graphene is the minimum gate-to-source voltage differential that is needed to create a conducting path between the source and drain terminals. From Eq. (11), the source-to-drain voltage $(V)_0^g$ is deduced as

$$(V_T)_0^g = \frac{k_\beta \tau V_F [6(1 + \exp(\beta\hbar\omega_q)) - \beta\hbar\omega_q(2 + \beta\hbar\omega_q \exp(\beta\hbar\omega_q))]}{e(2 - \beta\hbar\omega_q)(1 - \exp(-\beta\hbar\omega_q))}(\nabla T)_0^g. \quad (12)$$

Numerical analysis

To understand the complex expressions in Eqs. (9), (11) and (12), numerical method was adopted with the following parameters used: $\Lambda = 9$ eV, $V_s = 2.1 \cdot 10^3$ m/s, $\tau = 5 \cdot 10^{-10}$ s, $\omega_q = 1.5 \cdot 10^{12}$ s^{-1} and $q = 10^7$ m^{-1}. At $T = 77$ K, the calculated values for the threshold temperature gradient is $(\nabla T)_0^g = 746.8$ K/cm and threshold voltage $(V)_0^g = 6.6$ mV. Using these values, the Eq. (9) is analyzed numerically and presented graphically (see Figs. 1, 2). Figure 1(a) shows a normalized graph of Γ/Γ_0 on ω_q for varying ∇T. For $\nabla T = 550$ K/cm, it was observed that the amplitude of the absorption graph reduces and the absorption switches to amplification at $\omega_q = 10$ THz. Interestingly, when $\nabla T > (\nabla T)_0^g$, that is $\nabla T = 750$ K/cm and 950 K/cm, the graph switches completely to amplification ($\Gamma/\Gamma_0 < 0$) (see Fig. 1(a)). This agrees with the theory of thermoelectric amplification of phonons.

Figure 1(b) shows the graph of Γ/Γ_0 on various ∇T for varying ω_q. The graphs increases to a maximum then decreased with the peak shifting to the right for higher values of ω_q. This means the temperature gradient (∇T) attains a maximum at $\Gamma/\Gamma_0 > 0$ then decreases. A 3D graph is presented to further elucidate the graphs obtained (see Fig. 2). Figure 2 shows the dependence of Γ/Γ_0 on ∇T and ω_q. Along the ∇T axis, the graph increases to a maximum then decreases. On the ω_q axis, the graph attains a maximum at lower ∇T and a minimum at higher ∇T.

Conclusion

Thermoelectric amplification of in-plane phonons in graphenes is studied. We observed that absorption switches over to amplification at values greater than the threshold values. The threshold value calculated at $T = 77$ K in graphene is $(\nabla T)_0^g = 746.8$ K/cm and threshold voltage $(V_T)_0^g = 6.6$ mV. The threshold value is far higher than that calculated in homogeneous semiconductor using *n*-InSb ($V_s = 2.3 \cdot 10^5$ cm/s at 77 K) and was found to be $(\nabla T)_0^{\text{hom}} \approx \approx 10^3$ K/cm [21], superlattice $(\nabla T)_0^{SL} \approx 384$ K/cm for mini-band width $\Delta = 0.1$ eV at 77 K [24], and finally for cylindrical quantum wires (CQW) to be $(\nabla T)_0^{CWQ} \approx 10^2$ K/cm at liquid nitrogen temperature of 77 K [23]. These makes graphene a much better material for thermoelectric phonon amplification.

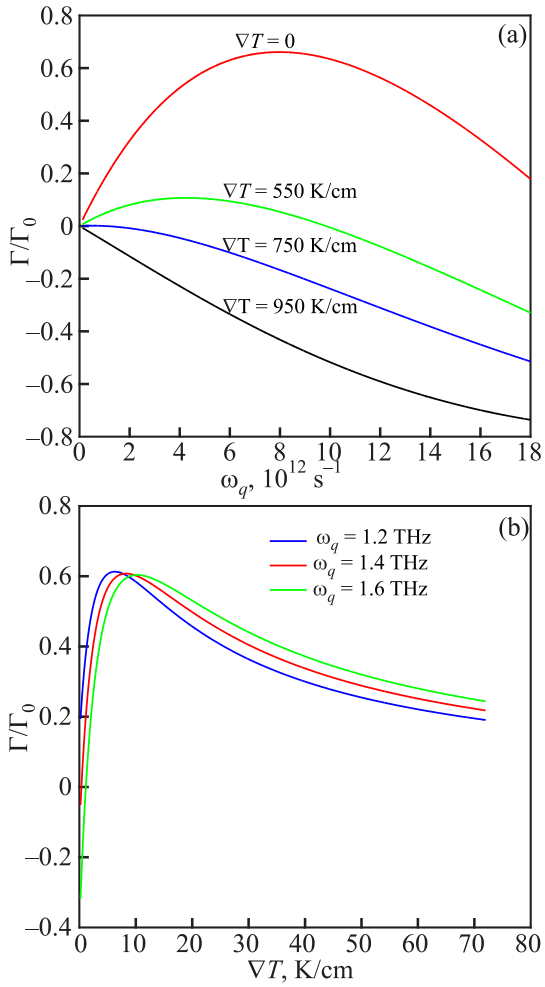

Fig. 1. The normalized graph of Γ/Γ_0 on ω_q for varying ∇T (a) and on ∇T for varying ω_q (b).

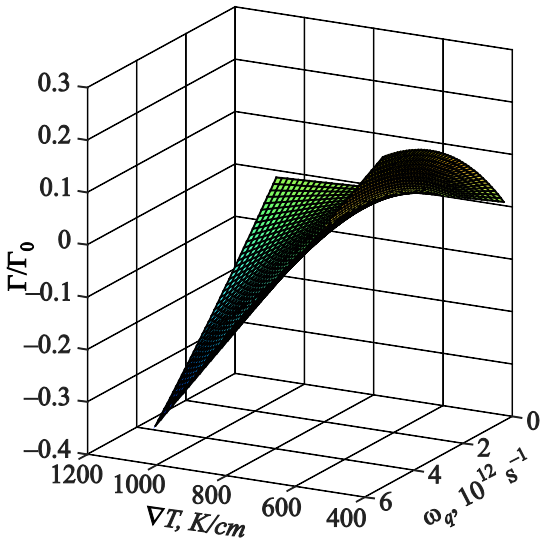

Fig. 2. (Color online) The dependence of Γ/Γ_0 on ω_q and ∇T.

1. A.C. Neto, F. Guinea, N.M.R. Peres, K.S. Novoselov, A.K. Geim, *Rev. Mod. Phys.* **81**(1), 109 (2009).
2. K.S. Novoselov, E. McCann, S.V. Morozov, V.I. Fal'ko, M.I. Katsnelson, U. Zeitler, D. Jiang, F. Schedin and A.K. Geim, *Nature Phys.* **2**, 177 (2006).
3. E. Mariani and F. von Oppen, *Phys. Rev. Lett.* **100**, 076801 (2008).
4. K.M. Borysenko, J.T. Mullen, E.A. Barry, S. Paul, Y.G. Semenov, J.M. Zavada, M. Buongiorno Nardelli, and K.W. Kim, *Phys. Rev. B* **81**, 121412(R) (2010).
5. K.A. Dompreh, N.G. Mensah, and S.Y. Mensah, *arXiv preprint arXiv:1505.05031* (2015).
6. K.A. Dompreh, S.Y. Mensah, S.S. Abukari, F. Sam, and N.G. Mensah, *arXiv preprint arXiv:1410.8064* (2014).
7. O.A.C. Nunes and A.L.A. Fonseca, *J. Appl. Phys.* **112**, 043707 (2012).
8. G.M. Shmelev, S.Y. Mensah, and G.I. Tsurkan, *J. Phys. C: Solid State Phys.* **21**, L1073 (1988).
9. S.Y. Mensah and G.K. Kangah, *J. Phys.: Condens. Matter* **3**, 4105 (1991).
10. S.Y. Mensah, F.K.A. Allotey, N.G. Mensah, and V.W. Elloh, *Physica E* **19**, 257 (2003).
11. K.A. Dompreh, S.Y. Mensah, N.G. Mensah, S.S. Abukari, F.K.A Allotey, and G.K. Nkrumah-Buandoh, *arXiv preprint arXiv:1101.1854* (2011).
12. K.A. Dompreh, N.G. Mensah, S.Y. Mensah, S.S. Abukari, F. Sam, and R. Edziah, *arXiv preprint arXiv:1502.07636* (2015).
13. N.Q. Hung, N.V. Nhan, and N.Q. Bau, *arXiv preprint cond-mat/0204563* (2002).
14. C.X. Zhao, W. Xu, and F.M. Peeters, *Appl. Phys. Lett.* **102**, 222101 (2013).
15. K.A. Dompreh, N.G. Mensah, and S.Y. Mensah, *arXiv preprint arXiv:1503.07360* (2015).
16. L. Bandhu, L.M. Lawton, and G.R. Nash, *Appl. Phys. Lett.* **103**, 133101 (2013).
17. S.Y. Mensah, F.K. A. Allotey, N.G. Mensah, and G. Nkrumah, *J. Phys.: Condens. Matter* **13**, 5653 (2001).
18. S.Y. Mensah, F.K.A. Allotey, N.G. Mensah, and G. Nkrumah, *Superlattices and Microstructures* **33**, 173 (2003).
19. S.Y. Mensah, A. Twum, N.G. Mensah, K.A. Dompreh, S.S. Abukari, and G. Nkrumah-Buandoh, a*rXiv preprint arXiv:1104.1913* (2011).
20. N.G. Mensah, G. Nkrumah, S.Y. Mensah, and F.K.A. Allotey, *Phys. Lett. A* **329**, 369 (2004).
21. Yu.V. Gulayev, *Phys. Lett. A* **30**, 260 (1969).
22. M.A. Tenan, A. Marotta, and L.C.M. Miranda, *Appl. Phys. Lett.* **35**, 321 (1979).
23. O.A.C. Nunes, D.A. Agrello, and A.L.A. Fonseca, *J. Appl. Phys.* **83**, 87 (1998).
24. S.Y. Mensah and G.K. Kangah, *J. Phys.: Condens. Matter* **4**, 919 (1992).
25. S. Sharma and S.P. Singh, *J. Appl Phys.* **10**, 46656-1 (1974).
26. E.M. Epstein, *Fiz. Tekh. Poluprov.* **8**, 1584-7 (1975).
27. S.Y. Mensah and G.K. Kangah, *J. Phys.: Condens. Matter* **3**, 4105 (1991).
28. A.A Balandin, *Nat. Mat.* **10**, 569 (2011).
29. N.S. Sankeshwar, S.S. Kubakaddi, and B.G. Mulimani, *Intech.* **9**, 1 (2013).